Mixed Convection at Supercritical Pressures

Marko Draskic, Jerry Westerweel, and Rene Pecnik

Abstract Fluids display sharp, non-linear variations of thermodynamic properties when they are heated at a supercritical pressure. As such, near-pseudo-critical heat transfer is often characterized by large variations in density, leading to sharp near-wall accelerations or strong stratifications when buoyancy becomes dominant. We study the modulation of heat transfer and turbulence by non-negligible buoyancy in such property-variant flows, for the development of near-pseudo-critical heat exchangers for supercritical energy conversion systems. In particular, a liquid-like, horizontal base flow of carbon dioxide at 88.5 bar and 32.6 $°C$ is considered, which is subjected to a vertical heat flux of up to 12.0 kW/m^2 at Reynolds numbers of up to $Re_{\mathrm{Dh}} \leq$ 10.000. Here, optical- and surface temperature measurements are used concurrently to evaluate the flow. Integratced visualizations of the flow field show the onset of strong stratifications with limited heating rates in the near-pseudo-critical region. During unstable stratification, the channel flow is dominated by the upward motion of thermal plumes. When the stratification is stable, any vertical motion and turbulence present in an equivalent neutrally buoyant flow is suppressed. As a result, wall heat is removed more effectively in the unstably stratified configuration than in a forced convective flow, whereas the opposite is true for a stably stratified flow. The difference in the perceived heat transfer between the considered configurations increases as buoyancy becomes more dominant.

Keywords Supercritical carbon dioxide · Stratification · Heat transfer · Shadowgraphy

M. Draskic (✉) · J. Westerweel · R. Pecnik
Process & Energy, ME, TU Delft, Delft, The Netherlands
e-mail: m.draskic@tudelft.nl

R. Pecnik
e-mail: r.pecnik@tudelft.nl

A. Giauque et al. (eds.), *Proceedings of the 5th International Seminar on Non-Ideal Compressible Fluid Dynamics for Propulsion and Power*, ERCOFTAC Series 32,
https://doi.org/10.1007/978-3-031-92695-2_15

1 Introduction

Beyond a fluid's critical point, the clear distinction between its liquid and gas phase disappears. When a fluid is heated at a supercritical pressure, it undergoes a bubble-free, boiling-like process. This pseudo-boiling leads to pronounced non-linear variations in thermodynamic properties, particularly near the pseudo-critical temperature (T_{pc}) where the specific heat capacity peaks. Several innovative energy conversion systems for the decarbonization of power and high-temperature industrial heat operate in the near-pseudo-critical region. The substantial variations in density that can be induced in the heat exchangers of these cycles, can lead to flows that are dominated by buoyant effects. Consequently, heat transfer in these systems is highly dependent on configuration and direction, with empirical rates varying significantly from ideal rates [1]. Unlike for systems with ideal fluids that follow the Oberbeck-Boussineq (OB) appromixation, this behavior does not require extreme temperature gradients but is instead induced at moderate heat transfer rates and temperature gradients at a supercritical pressure (Fig. 1).

The stratification type, determined by the direction of the vertically imposed density gradient, plays a critical role in heat transfer when buoyancy is non-negligible. In unstable stratification a lighter fluid is formed below denser fluid in a bottom-upward heated flow, creating warm plumes and cold downdrafts. Here, the increased upward transfer of momentum enhances turbulence and wall-fluid heat transfer compared to a forced convective flow [2, 3]. Conversely, in stable stratification, where lighter fluid is formed above a denser bulk during downward heating, vertical movement is suppressed, reducing turbulent mixing and heat transfer efficiency [4–6]. This suppression occurs because the potential energy required to displace fluid parcels vertically is unmet along a density gradient, leading to elongated thermal structures aligned with the flow direction and decreased near-wall turbulence [6–8].

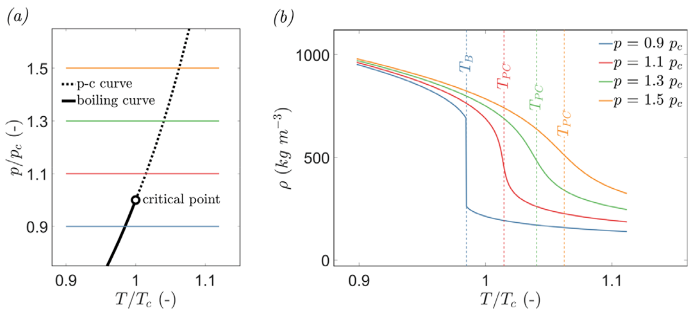

Fig. 1 The density of carbon dioxide, for which $T_c = 31.0°C$ and $p_c = 73.8$ bar, is shown in **b** for the isobaric heating processes shown in **a**. The pseudo-critical (p-c) curve is defined at the local maxima of the specific heat c_p. The p-c curve embodies the informal boundary between liquid-like carbon dioxide (to the left of the curve) with gas-like carbon dioxide (on the right)

The stable and unstable stratification of mixed convective flows is well-documented under the Oberbeck-Boussinesq approximation, or with linearly varying thermodynamic properties. However, discussions on the strong stratification with fluids with sharp, non-linear variations in thermodynamic properties are limited, particularly in an experimental context. It is however in systems with such fluids in particular, for which strong stratifications most readily prevail in practical applications.

In our work, horizontal flows of carbon dioxide at supercritical pressure with non-negligible buoyancy are experimentally explored, to predict and optimize the performance of heat exchangers of energy conversion systems at supercritical pressures. In particular, hydrodynamically developed horizontal channel flows to which one-sided vertical heating is imposed are considered. The channel can be heated in both bottom-up and top-down configurations, allowing the examination of both stable and unstable stratifications. In the our experimental facility, optical measurements are used concurrently with surface temperature measurements to study the flow at high temporal resolutions, overcoming the limitations of thermal inertia in the pressure vessel walls.

2 Methodology

The test section used to perform optical experiments with carbon dioxide in this work is shown schematically in Fig. 2. The test section is part of a larger experimental facility, in which carbon dioxide is circulated naturally in a vertically oriented closed flow loop. In the test section, bilateral optical access is provided to a rectangular channel using tempered borosilicate visors. At the streamwise location of the sight glasses, a unidirectional and constant vertical heat flux is applied to the channel. By inverting the test section, the heating can be applied in either vertical direction. In both configurations, the temperature of the heated surface is measured locally, using K-type thermocouple probes with a nominal uncertainty of $\pm 0.5°C$. The thermodynamic condition at the test section inlet is evaluated with a resistance

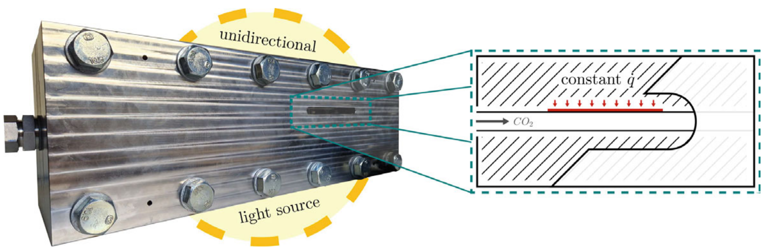

Fig. 2 Image of current test section (left) with schematic partial cross section of test section channel (right). A collimated light source is positioned behind the test section, creating a variable brightness shadowgram on the other side of the test section when the carbon dioxide is property-variant and turbulent. The rectangular test section channel is locally heated in a single vertical direction

thermometer bulk temperature measurement with a nominal accuracy of $\pm 0.1°C$, and an absolute pressure measurement with a nominal uncertainty of ± 0.16 bar or 0.1%. The thermocouples are calibrated and shifted against the readings of the resistance transmitter in situ. The imposed steady state mass flow rate $\dot{m}$ is evaluated from the enthalpy difference over the heated vertical leg of the natural circulation facility. The uncertainty of the shown results is evaluated by assuming the independence of the respective variables measured by the transmitters in the system, allowing for the propagation of their respective errors.

A collimated-LED shadowgraphy setup is used to yield shadowgrams in this work. Here, a variable-brightness image is projected by an initially parallel light bundle after it passes the non-ideal carbon dioxide. Images are recorded using a Pixelink PL-D755MU-T CMOS camera (2448 × 2048 pixels, monochromatic). The exposure time of the sensor is maintained at 20 µs for all shadowgrams. Furthermore, the contrast of each image is stretched to cover the full brightness range.

3 Results

Instantaneous shadowgrams of an unheated, neutrally buoyant flow of carbon dioxide at supercritical carbon dioxide are shown in Fig. 3. The shadow cast on the image plane by the property-variant carbon dioxide reveals the presence of irregular thermal structures along the width of the channel. When the carbon dioxide is turbulent, its naturally present variations in refractive index show the motion of depth-integrated thermal structures in the shadowgram. As such, a comparison of the consecutive shadowgrams in Fig. 3 allows for the seedless visualization of the flow field [9, 10]. The resulting flow field is non-planar, as the refractive index is integrated across the channel. Therefore, its interpretability diminishes in the large Reynolds number limit; when many smaller thermal structures overlap laterally, or when structures

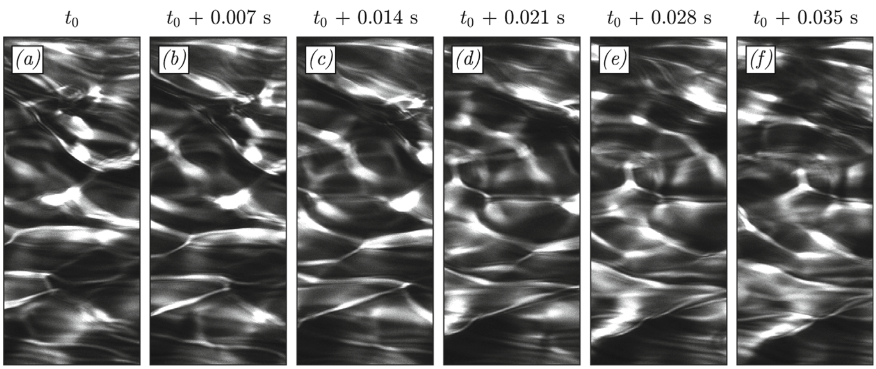

Fig. 3 Consecutive shadowgrams in a neutrally buoyant, unheated flow of carbon dioxide. Here, $Re_{Dh} = 3.8 \cdot 10^3$, $p = 88.5$ bar, $T_b = 32.6°C$

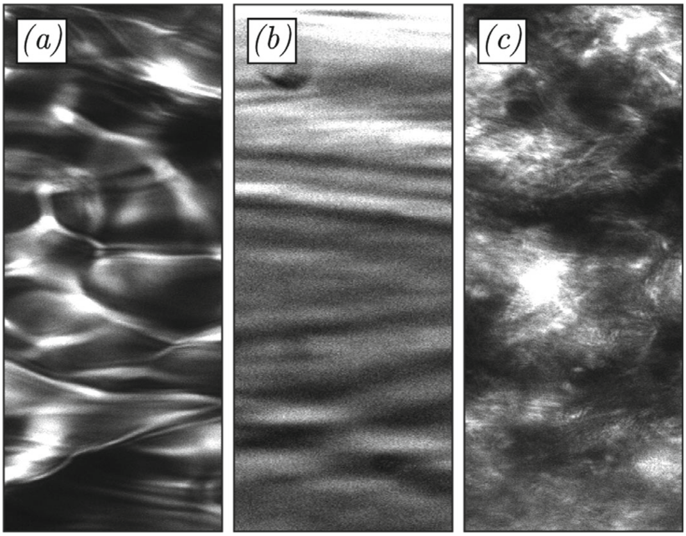

Fig. 4 Comparison of an unheated flow in **a**, a top-heated flow in **b**, and a bottom-heated flow in **c**. Here, $Re_{Dh} = 3.8 \cdot 10^2$, $p = 88.5$ bar, $T_b = 32.6$°C. The imposed wall-normal heating rate in both **b** and **c** is $\dot{q} = 12.0$ W/m^2

dissipate quickly. Furthermore, the reconstructed flow field undercaptures the actual fluid velocity in the low Reynolds number limit, as less inhomogeneous turbulent thermal tracer parcels are present to visualize the flow field with. Nevertheless, the current shadowgrams show distinguishable mean and instantaneous movement at all planes across the channel simultaneously for a band of Reynolds numbers.

Figure 4 shows a comparison between a neutrally buoyant, unheated flow, a flow that is heated in a stably stratified configuration, and a flow that is heated in an unstably stratified configuration. The thermodynamic condition and mass flow rate is constant for all three considered cases. Under strong top-down heating ($\dot{q} = 12.0$ W/m^2), the thermal structures originally present in the neutrally buoyant flow are elongated in the streamwise direction and disappear in the shadowgrams. Any vertical motion in the near-wall region is furthermore suppressed. As such, the resulting shadowgrams are mostly homogeneous in both space and time. When the flow is heated in a bottom-up setting ($\dot{q} = 12.0$ W/m^2), the optical signal is dominated by the upward movement of thermal plumes across the channel. Figure 5 shows the inception of thermal plumes after bottom-up heating is commenced for a laminar base flow. In the buoyancy dominant limit, the irregular and intermittent structures overlap laterally, and vertical movement is difficult to distinguish in the resulting blurry shadowgrams. Nevertheless, the upward momentum transfer is discernible under mixed convection and moderate heating rates within the considered range.

The considered shadowgrams show significantly different trends between the two considered stratification types. Under unstable stratification, increased momentum transfer is perceived, away from the heated wall towards the bulk of the flow. On

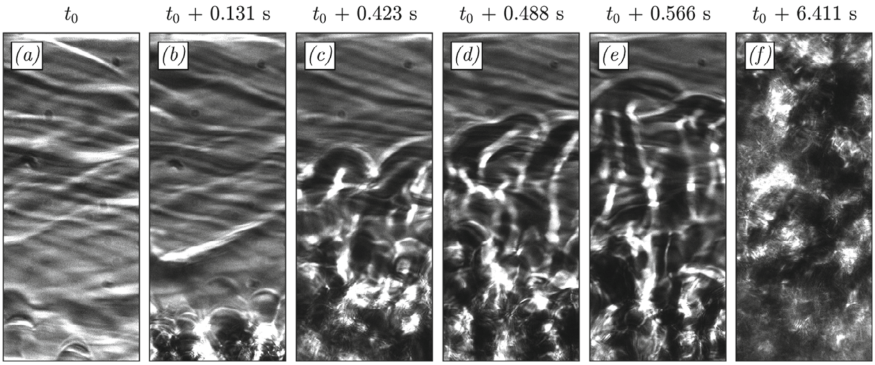

Fig. 5 Consecutive shadowgrams in an unstably stratified, bottom-heated flow of carbon dioxide show the upward ejection of low-density thermal plumes. Here, $Re_{Dh} = 1.0 \cdot 10^3$, $p = 88.5$ bar, $T_b = 32.6°C$, $\dot{q} = 12.0$ W/m^2. At $t = t_0$, the bottom-up heating is commenced

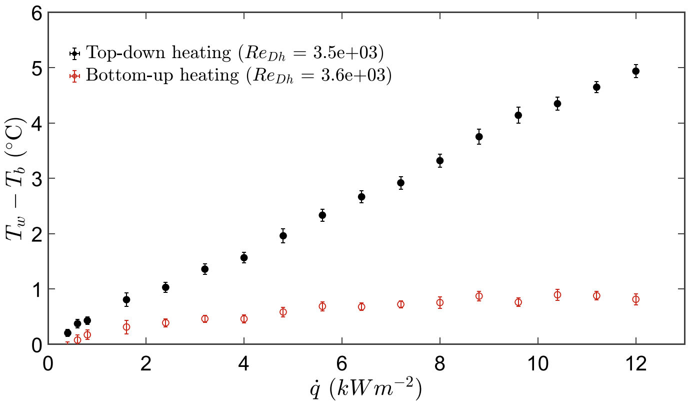

Fig. 6 The difference between wall- and bulk temperatures T_w and T_b for the cases shown in Fig. 4. The black data points show a stably stratified flow, whereas data of an unstably stratified flow is shown with red, unfilled markers

the contrary, when the flow is stably stratified, most vertical motion is suppressed. Figure 6 shows that the modulation in vertical momentum transfer in either stratification type results in an equivalent change of the heat transfer rate. At a constant heating rate for a buoyancy-dominated channel flow, heat is removed more effectively in the unstably stratified configuration. For the cases shown in Fig. 4, an up to five fold difference of the wall-temperature increase is found between the two considered vertical heating configurations. In an equivalent setting with an ideal fluid, the buoyant contribution would be negligible, and no significant difference in the heat transfer rates of the two considered configurations would be found.

4 Conclusions and Future Works

This work presents a preliminary optical investigation of a horizontal channel flow of carbon dioxide at supercritical pressure. The flow is heated vertically to incite both stable and unstable stratifications. Shadowgraphy is used to image fluid motion across the considered channel. Here, shadowgrams show increased upward motion in the unstably stratified configuration, in which buoyancy is non-negligible. As the vertical momentum transfer rate increases, the wall-normal heat transfer rate increases accordingly for the parameter range considered in this work. When the flow is heated in a stably-stratified configuration, both wall-normal motion and turbulent structures are suppressed in the near-wall region. As a result, the heat removal rates in the unstably stratified configuration far exceed those in a stably stratified arrangement.

References

1. Wang, Q., Jinliang, X., Zhang, C., Hao, B., Cheng, L.: A critical review on heat transfer of supercritical fluids. Heat Transf. Eng. **44**(21–22), 1969–1994 (2023)
2. Garai, A., Kleissl, J., Sarkar, S.: Flow and heat transfer in convectively unstable turbulent channel flow with solid-wall heat conduction. J. Fluid Mech. **757**, 57–81 (2014)
3. Pirozzoli, S., Bernardini, M., Verzicco, R., Orlandi, P.: Mixed convection in turbulent channels with unstable stratification. J. Fluid Mech. **821**, 482–516 (2017)
4. Ohya, Y., Neff, D.E., Meroney, R.N.: Turbulence structure in a stratified boundary layer under stable conditions. Boundary-Layer Meteorol. **83**, 139–162 (1997)
5. García-Villalba, M., Del Alamo, J.C.: Turbulence modification by stable stratification in channel flow. Phys. Fluids **23**(4) (2011)
6. Williams, O., Hohman, T., Van Buren, T., Bou-Zeid, E., Smits, A.J.: The effect of stable thermal stratification on turbulent boundary layer statistics. J. Fluid Mech. **812**, 1039–1075 (2017)
7. Smith, K.M., Caulfield, C.P., Taylor, J.R.: Turbulence in forced stratified shear flows. J. Fluid Mech. **910**, A42 (2021)
8. Zonta, F., Sichani, P.H., Soldati, A.: Interaction between thermal stratification and turbulence in channel flow. J. Fluid Mech. **945**, A3 (2022)
9. Jonassen, D.R., Settles, G.S., Tronosky, M.D.: Schlieren “piv” for turbulent flows. Opt. Lasers Eng. **44**(3–4), 190–207 (2006)
10. Hargather, M.J., Lawson, M.J., Settles, G.S., Weinstein, L.M.: Seedless velocimetry measurements by schlieren image velocimetry. AIAA J **49**(3), 611–620 (2011)